Liquid Crystals
Publication details, including instructions for authors and subscription information:
http://www.informaworld.com/smpp/title~content=t713926090

The molecular aspect of the double absorption peak in the dielectric spectrum of the antiferroelectric liquid crystal phase

M. Buivydas[a]; F. Gouda[a]; S. T. Lagerwall[a]; B. Stebler[a]
[a] Physics Department, Chalmers University of Technology, Göteborg, Sweden

To cite this Article Buivydas, M. , Gouda, F. , Lagerwall, S. T. and Stebler, B.(1995) 'The molecular aspect of the double absorption peak in the dielectric spectrum of the antiferroelectric liquid crystal phase', Liquid Crystals, 18: 6, 879 — 886
To link to this Article: DOI: 10.1080/02678299508036706
URL: http://dx.doi.org/10.1080/02678299508036706

LIQUID CRYSTALS, 1995, VOL. 18, NO. 6, 879–886

The molecular aspect of the double absorption peak in the dielectric spectrum of the antiferroelectric liquid crystal phase

by M. BUIVYDAS, F. GOUDA*, S. T. LAGERWALL and B. STEBLER
Physics Department, Chalmers University of Technology S-412 96, Göteborg, Sweden

(*Received 18 September 1994; accepted 18 November 1994*)

The dielectric spectrum of the antiferroelectric smectic C* phase exhibits a low and a high frequency absorption peak (P_L, P_H) which have been studied as a function of temperature and bias electric field. Measurements from 10 Hz to 10 MHz were carried out with smectic layers parallel and quasi-perpendicular to the cell plates for the multicomponent mixture CS-4000 (Chisso). In addition to the orthogonal smectic A* phase, this material has four tilted phases, three narrow phases with a dielectric behaviour permitting us to classify two of them as C_α^* (82·80° to 81·91°C) and C_γ^* (80·10° to 79·17°C), and one broad antiferroelectric phase (79·17° to − 10°C). On applying an increasing bias field, $\Delta\varepsilon$ for both processes first increases by about a factor of two, then exhibits a maximum at a threshold field E_C corresponding to the antiferroelectric–ferroelectric transition at which it decreases by almost one order of magnitude. In fact, at E_C the P_H peak vanishes and the P_L peak shows up at a frequency slightly lower than that corresponding to zero field. In contrast to the $\Delta\varepsilon$ behaviour, the relaxation frequency of the two absorptions does not show any appreciable bias field dependence for $E < E_C$. We attribute the P_H process to the collective reorientation of the molecules around the cone in the *opposite* direction (anti-phase in the φ variable). P_L may be attributed to a similar collective reorientation in the same direction (in-phase) around the cone, where the coupling to the electric field is mediated by the helical superstructure, and a corresponding small shift in the local polarization directions. There is no antiferroelectric soft mode coupling to an electric field, but the anti-phase cone motion acts electro-optically in a way similar to the electroclinic effect.

1. Introduction

Dielectric relaxation spectroscopy has proven to be a powerful technique to study the dipolar ordering and molecular dynamics of collective and non-collective molecular processes in paraelectric, ferroelectric [1–10] and antiferroelectric [11–19] chiral smectic liquid crystals. In the paraelectric A* phase, the dielectric permittivity ε has a contribution from the director tilt fluctuations (soft mode). In the ferroelectric chiral C* phase, ε has, besides the soft mode, another mode due to phase fluctuations (Goldstone mode). The Goldstone mode is characterized by a relaxation frequency which, for most compounds investigated so far, does not exceed 1 kHz. On approaching the A* to C* transition, the soft mode dielectric strength ($\Delta\varepsilon_S$) diverges and its relaxation frequency (f_S) exhibits a critical slowing down. The Goldstone mode dielectric strength ($\Delta\varepsilon_G$), except in the vicinity of the A* to C* transition, is larger than that of the soft mode by two orders of magnitude. Thus, resolving the soft mode dielectric contribution in the C* phase requires somehow the removal of the Goldstone mode. By applying a bias electric field, the helical structure can be unwound, thereby quenching the dielectric contribution of the Goldstone mode. In this way [20], the soft mode dielectric behaviour has been studied over a wide temperature interval in the C* phase.

The dielectric spectrum of the antiferroelectric smectic C* (C_A^*) phase exhibits two absorption peaks (P_L, P_H) [16, 17] observed in the kHz and MHz range, respectively. The dielectric strength ($\Delta\varepsilon$) of these two modes is less than $\Delta\varepsilon$ of other absorptions, like the soft mode in the A* and C* phases, by at least one order of magnitude. The temperature dependence of dielectric strength and relaxation frequency (f_H) of the P_H process in the C_A^* phase depends, to a certain extent, on the adjacent high temperature phase. For instance, at the onset of C_A^* preceded by an A* phase, the value of f_H exhibits a sharp increase with decreasing temperature followed, on further cooling, first by a broad maximum and then a pronounced decrease. However, when the C_A^* phase is preceded by a C* phase, the value f_H is almost temperature independent. The dielectric strength of the P_L and P_H modes exhibits, except over a narrow temperature interval, a slight increase with decreasing temperature.

---

* Author for correspondence.

0267-8292/95 $10·00 © 1995 Taylor & Francis Ltd.

It has been reported that by applying a bias electric field, a third absorption peak can be resolved [16, 17] in the dielectric spectrum of the $\mathrm{C}_{\mathrm{A}}^*$ phase. While the molecular aspect of the P_{L} and P_{H} modes is still a subject of controversy, the third process observed in the presence of a bias electric field has been attributed to an 'induced Goldstone mode'. In [16], the P_{H} process has been interpreted as a soft mode; however, other authors [17] have attributed this process to the distortion of the antiferroelectric ordering—the reorientation of the molecules in two adjacent smectic layers in an *opposite* unwinding fashion. The P_{L} mode is assigned [16, 17] to a 'non-collective' molecular reorientation around the short axis, a process which is usually observed in the quasi-homeotropic orientation of tilted smectics. In the present work, the frequency, temperature and bias field dependence of the complex dielectric permittivity has been studied in the A*, C_{α}^*, C_{γ}^* and $\mathrm{C}_{\mathrm{A}}^*$ phase, with emphasis on the last. The aim is to clarify the molecular origin of the P_{L} and P_{H} processes. We can identify the phason nature of the high frequency mode and find likewise the low frequency mode corresponding to a third absorption.

2. Experimental

The dielectric measurements from 10 Hz to 10 MHz were carried out for planar and homeotropic geometries—with reference to the A* phase—of the Chisso mixture CS-4000. According to Chisso, the material has a transition from isotropic to A* at 100°, from A* to C* at 84° and from C* to $\mathrm{C}_{\mathrm{A}}^*$ at 82°C. The $\mathrm{C}_{\mathrm{A}}^*$ phase persists down to $-10°$. Measured at 25°C, the tilt angle θ is 27°, the local polarization P_{S} 79·8 nC cm^{-2} (dipole density of one layer) and the threshold for the field-induced transition to the ferroelectric state 9·8 V µm^{-1}. Our transition temperatures and phase designations, based on the dielectric behaviour, turned out to be slightly different and this will be discussed further below. In the planar case, a measuring electric field of 0·3 $\mathrm{V_{PP}}$ was applied across the sample, usually in a direction parallel to the original smectic layers. In order to study the electric field dependence of the dielectric permittivity and relaxation frequency, a bias electric field of (0 to ±35 V) was superimposed on the internal field from the HP-4192 bridge. The cell consists of two glass plates each coated with a conducting layer (indium tin oxide, ITO). Two thin layers of silicon monoxide have further been evaporated. The first layer is evaporated normal to the surface and used as an insulation layer to avoid the breakdown of the cell at high fields. The second layer is obliquely evaporated in order to achieve the planar orientation (which is facilitated by an additional weak shear). The dielectric measurements, in the planar orientation, have been carried out on three cells of 2 µm, 18 µm and 36 µm thickness. By applying, in the A* phase, a strong and high amplitude (~1 mm) shear on the 2 µm cell, the planar orientation was easily transformed into the quasi-homeotropic orientation.

In different chiral smectics, the complex dielectric permittivity ε^* depends on the frequency (f) of the measuring electric field, the temperature (T) and the bias electric field (E). We may write $\varepsilon^*\ (f, T, E)$ as

$$\varepsilon^*(f,T,E) = \frac{\Delta\varepsilon_{\mathrm{L}}(T,E)}{1+\left(j\dfrac{f}{f_{\mathrm{L}}(T,E)}\right)^{1-\alpha_{\mathrm{L}}}} + \frac{\Delta\varepsilon_{\mathrm{H}}(T,E)}{1+\left(j\dfrac{f}{f_{\mathrm{H}}(T,E)}\right)^{1-\alpha_{\mathrm{H}}}} + \varepsilon(\infty) \qquad (1)$$

where $\Delta\varepsilon_{\mathrm{L}}$, $\Delta\varepsilon_{\mathrm{H}}$, f_{L}, f_{H} and α_{L}, α_{H} refer to the dielectric strengths, relaxation frequencies and symmetric distribution parameters of P_{L} and P_{H} in the $\mathrm{C}_{\mathrm{A}}^*$ phase. The high frequency dielectric permittivity $\varepsilon(\infty)$ has contributions from the molecular reorientation around the long axis [10] and other high frequency processes. The dielectric strength $\Delta\varepsilon$ of each mode is defined as the difference ($\Delta\varepsilon = \varepsilon(0) - \varepsilon(\infty)$) between the dielectric permittivity measured at low and high frequencies of a relaxation region.

The measured dielectric absorption ε'' contains, besides the double absorption peaks, a spurious contribution in the high frequency part of the spectrum due to the resistance of the ITO layer for which correction must be made (see figure 1). In order to extract the correct values of $\Delta\varepsilon_{\mathrm{L}}$, $\Delta\varepsilon_{\mathrm{H}}$, f_{L}, f_{H}, α_{L} and α_{H}, the imaginary part of the measured frequency dependence of ε'' has been fitted to two

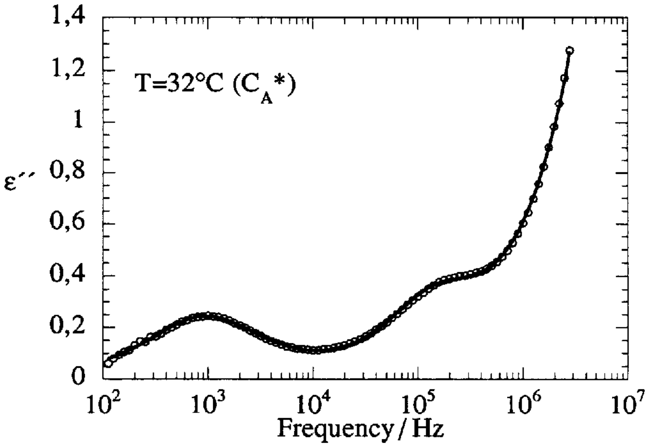

Figure 1. Frequency dependence of the dielectric absorption. The solid line represents the fitting of equation (2) to the experimental results.

absorption peaks of Cole–Cole type

$$\varepsilon'' = \mathrm{Im}\left(\frac{\Delta\varepsilon_L}{1+\left(j\dfrac{f}{f_L}\right)^{1-\alpha_L}} + \frac{\Delta\varepsilon_H}{1+\left(j\dfrac{f}{f_H}\right)^{1-\alpha_H}} + \varepsilon(\infty)\right) + Af^n \qquad (2)$$

where A and n are fitting parameters of the high frequency contribution arising from the ITO layer. The factor A depends on the time constant $\tau(\tau = RC)$ of our cell, originating in the resistance R of the ITO layer and the capacitance C of the capacitor. For thinner cells, the cut-off frequency (or $1/\tau$) will be lower than for thicker cells. This means that the contribution from the term Af^n in equation (2) will be more dominating at lower frequencies and eventually may obscure an absorption peak due to a molecular process. In our case, the dielectric measurements have been carried out on 2 μm, 18 μm and 36 μm thick cells. In general, the results were found to be reproducible. However, in the thicker cells, where the cut-off frequency is shifted to a much higher range of the spectrum, the results are more accurate and therefore will, unless otherwise mentioned, be presented in this paper. Another common problem in dielectric measurements is the transport of the freely moving charges resulting in an additional contribution to ε'' at low frequencies. In our case, this contribution was not taken into account in the fitting procedure because the ionic contribution was found to be negligibly small, and also the values of ε'' below 100 Hz fluctuate to the extent that including them in the fitting procedure would only increase the uncertainty in the fitting parameters.

3. Results and discussion

3.1. *Evidence from planar samples*

Figure 2 shows an illustrative example of the frequency dependence of the dielectric absorption in the frequency range 10^2 to 10^7 Hz. In the A* phase, the dielectric spectrum contains one peak, whereas the spectrum of the C$_A^*$ phase exhibits two absorption peaks P_L and P_H separated by two frequency decades. The dielectric strength of P_L and P_H is much smaller than in the A* phase. The temperature dependence of the dielectric strength and the relaxation frequency in the different phases are depicted in figure 3. In the A* phase, the relaxation frequency exhibits the expected slowing down behaviour with decreasing temperature, and the dielectric strength shows a diverging-like behaviour when approaching the A* to C$_\alpha^*$ transition temperature T_C. This temperature dependence is typical for a soft mode. It may be noted that at T_C, the cut-off frequency is about 10 kHz, a value which is much higher than that usually obtained in compounds which do not possess an antiferroelectric phase [8, 20].

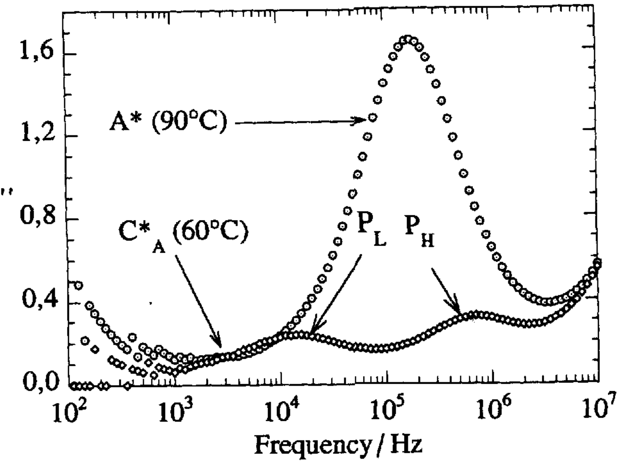

Figure 2. Frequency dependence of the dielectric absorption in the A* and C$_A^*$ phases.

Within the three intermediate phases C$_\alpha^*$, C$_x^*$ and C$_\gamma^*$, (where C$_x^*$ describes a tilted phase of unknown nature) between the A* and the C$_A^*$ phase, the dielectric strength decreases with decreasing temperature, and the relaxation frequency increases. This behaviour is typical for the soft mode of a low temperature phase. In the temperature interval 82·80° to 81·91°C, the behaviour of Δε and f_R with temperature is similar to that reported for the C$_\alpha^*$ phase [12–15]. From our measurements in the phase region between 80·10° to 79·17°C, the dielectric spectrum exhibits, besides the soft mode, an additional low frequency absorption peak (centred around 15 Hz and not shown in Figure 3 (*a*)) with a large value of dielectric strength (see sub figure 3 (*b*)). This phase may either be the ferroelectric C* phase or the ferrielectrc C$_\gamma^*$ phase, both possessing a Goldstone mode [20, 21]. However, since the observed dielectric strength of the Goldstone mode, in this case, is not as large as the one usually observed in the ferroelectric C* phase, we may designate the phase region 80·10° to 79·17°C as the ferrielectric C$_\gamma^*$ phase. The dielectric behaviour observed in the temperature interval (81·91° to 80·10°C) between the C$_\alpha^*$ and C$_\gamma^*$ phases does not permit, at the present stage, the identification of this phase. Therefore it is denoted as C$_x^*$. At the onset of the antiferroelectric phase, the relaxation frequency splits up into two branches representing the high and low frequency absorption peaks of the C$_A^*$ phase. The latter has a much more pronounced temperature dependence than the former. The high frequency absorption peak in the C$_A^*$ phase has none of the characteristics of a soft mode, rather the contrary: $\Delta\varepsilon_H$ is increasing with decreasing temperature, whereas f_H is decreasing (see figure 3 (*a*) and (*c*), respectively.) It therefore cannot be associated with a soft mode as proposed in [16]. The low frequency absorption has been attributed, by different authors [16, 17] to a non-collective reorientation around the short axis. We will below present evidence as to why we believe that his assignation is equally inadequate.

In order to facilitate the identification of different phases, conoscopic measurements were made on a 2 μm thick sample (in order to achieve a non-helicoidal state starting from the A* phase, through the C^*_α phase into the C^*_A phase. No change was seen in the uniaxial picture at the A*–C^*_α at 82·8° confirming the interpretation of the C^*_α as antiferroelectric. However, the conoscopic cross shifted to biaxial at 80·10° (C^*_γ), returning to uniaxial at 79·17°C.

3.2. *Evidence from quasi-homeotropic samples*

The best way to probe the reorientation around the short molecular axis is to prepare a smectic A* sample in the homeotropic orientation (layers parallel to the glass plates). In this geometry the relaxation frequency f_{hom} has the temperature dependence given in figure 4 (*a*), where it is compared with that of the low frequency mode in the C^*_A phase, f_L. From the geometry, it is clear that we are strictly probing the reorientation around the short axis as long as we are in the A* phase. From the continuity through the A*, C^*_α, C^*_γ, C^*_x and C^*_A phases, it is further clear that the same motion is probed in all three phases. The temperature dependence (as well as the actual values of f_R) confirms that it is not a question of a soft mode, but a non-collective rotation around the short axis. We are therefore in a position to exclude that f_L represents such a motion, because it has a different frequency. In fact, the difference amounts to a factor of two. Further evidence can be obtained from a comparison of the dielectric strength $\Delta\varepsilon_L$ with that measured in the homeotropic orientation $\Delta\varepsilon_{\mathrm{hom}}$, see figure 4 (b). We note from figure 4 (b) that $\Delta\varepsilon_{\mathrm{hom}}$ is larger than $\Delta\varepsilon_L$. However, it would be hard to imagine how $\Delta\varepsilon_L$ could be constant or even decreasing with decreasing temperature if it were to describe the short axis reorientation, given the fact that with increasing tilt angle an even larger part of the electric field is acting along the molecular axis. We have carried out yet another set of measurements in order to prove that the P_L process cannot be connected with the molecular reorientation around the short axis. Figure 4 (*c*) shows the dielectric absorption from three measurements carried out, at the same temperature, 62·0°C, in two different measurement geometries. The first measurement (curve 1)) was performed with the quasi-homeotropic orientation, and the spectrum contains the expected absorption peak arising from the molecular reorientation around the short axis. The sample was then heated up into the isotropic phase and slowly cooled down to the A* phase. Now, fairly good planar orientation was obtained due to the influence of the surface treatment discussed earlier. The sample was cooled down further to 62·0°C and the second measurement was performed as

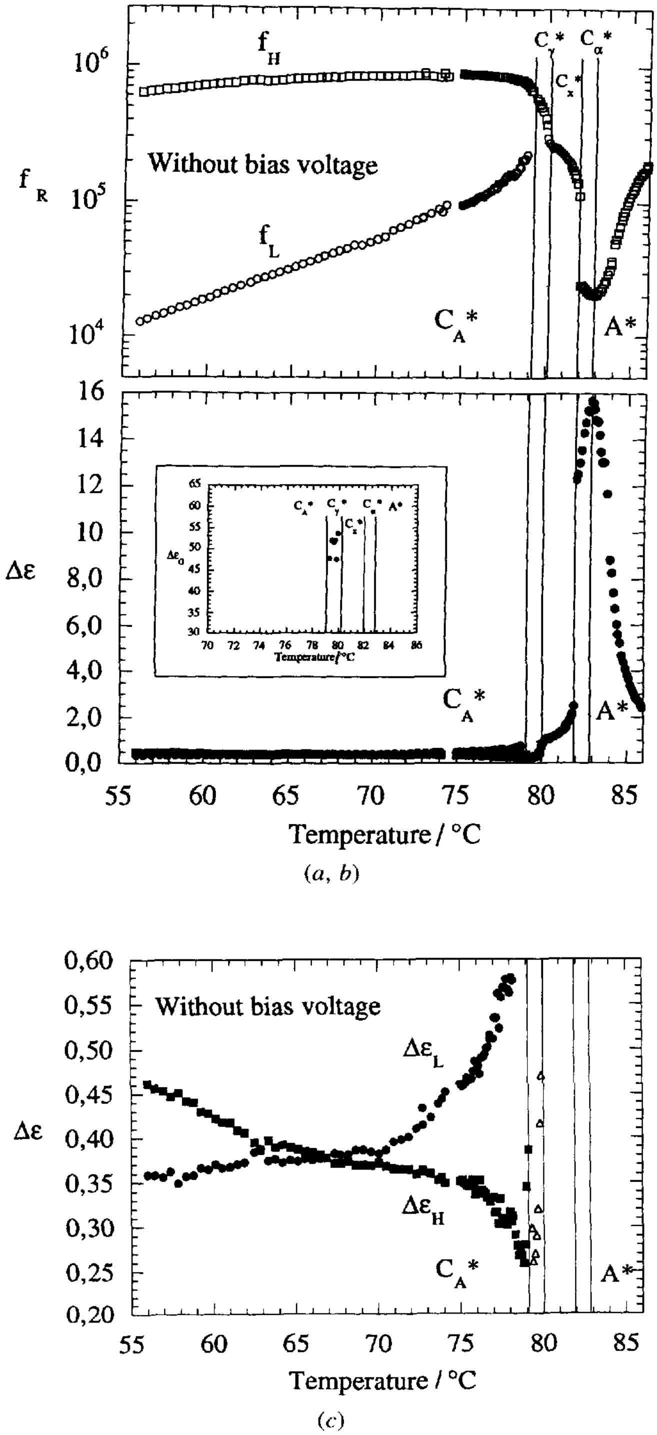

(*a*, *b*)

(*c*)

Figure 3. Temperature dependence of the relaxation frequencies (*a*) and dielectric strength (*b*) measured for the A*, C^*_α, C^*_x, C^*_γ and C^*_A phases. The temperature dependence of the Goldstone mode in the ferrielectric C^*_γ phase is depicted on a larger scale in the sub-fig. of figure 3 (*b*). There are two modes in the C^*_γ phase. The points on the sub-figure 3 (*b*) are scattered because the corresponding absorption peak is observed at a very low frequency. Temperature dependence of the dielectric strength of the P_H and P_L process (*c*).

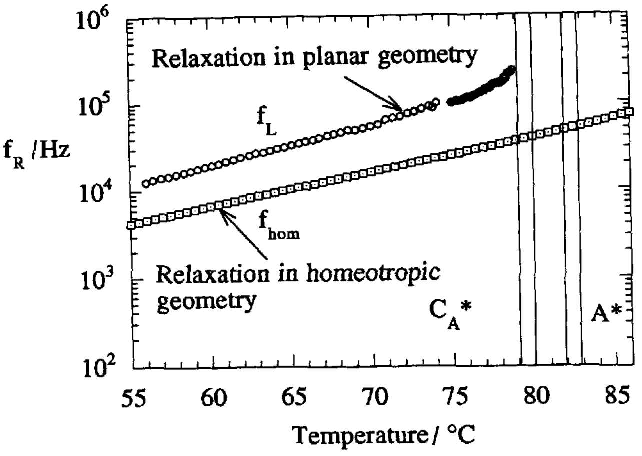

(*a*)

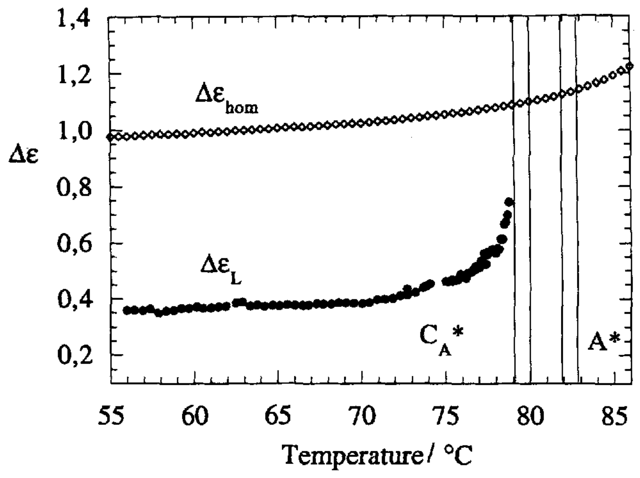

(*b*)

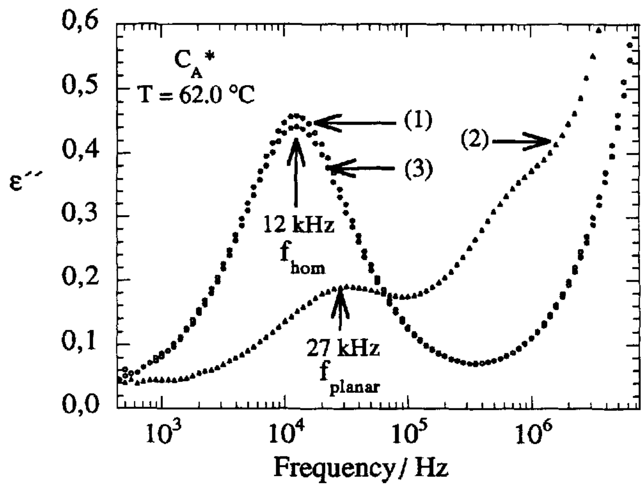

(*c*)

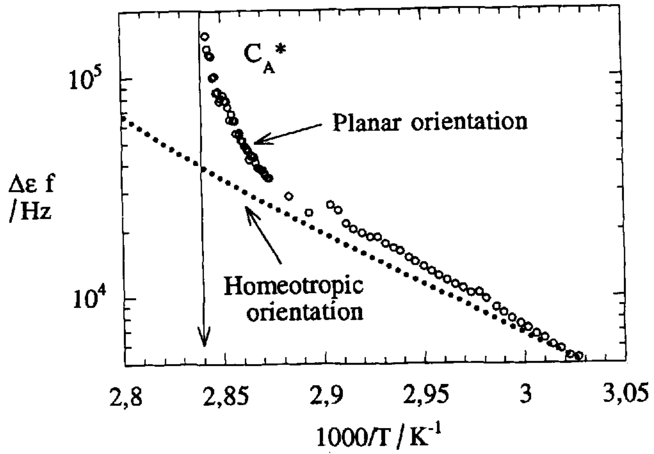

(*d*)

Figure 4. (*a*) Comparison of the temperature dependence of the relaxation frequency f_L measured for the planar orientation and the relaxation frequency f_{hom} of the molecular reorientation around the short axis measured for the homeotropic orientation. (*b*) Temperature dependence of the dielectric strength $\Delta\varepsilon_L$, and of the dielectric strength $\Delta\varepsilon_{hom}$ measured for the homeotropic orientation. (*c*) Frequency dependence of the dielectric absorption in the C_A^* phase measured for homeotropic (curves (1) and (3)) and planar (curve (2)) orientations. (*d*) Arrhenius plot of the product $\Delta\varepsilon f_R$ determined from measurements performed for the planar (low frequency peak) and homeotropic (rotation around short axis) geometries.

given by the curve (2). The spectrum for this orientation exhibits the double absorption peaks P_H and P_L. By applying a strong shear on the cell, at the same temperature, an excellent quasi-homeotropic orientation was finally obtained again. This allows us to perform the third measurement, on the same cell, in the homeotropic orientation, as given by curve (3). In this measurement geometry, the absorption peak representing the molecular reorientation around the short axis coincides with that obtained in the first run. In fact, if the P_L process were connected with the molecular reorientation around the short axis, one would expect the position of the peaks (f_L and f_{hom}) to coincide with each other. Finally, some interesting information can be obtained by multiplying f_R by $\Delta\varepsilon$. As is well known, the product $f_R\Delta\varepsilon$ is, within a large range of validity, equal to a constant times the inverse of the corresponding viscosity. From the plot of $f_R\Delta\varepsilon$ in figure 4 (*d*) we learn that the low frequency absorption behaves differently from the short axis reorientation in the sense that it diverges towards the upper end of the phase, which means that the viscosity gets very small. This is a well-known behaviour of the rotational viscosity for the motion around the smectic cone when the cone angle gets very small. Hence, this is a direct indication that the low frequency peak arises from fluctuations in the phase variable.

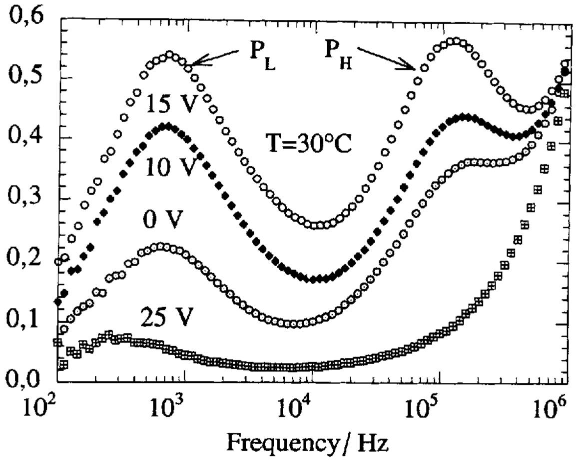

Figure 5. Frequency dependence of the dielectric absorption in the C^*_A phase measured at different bias fields. The bias field measurements have been carried out on a thin sample of 2 μm thickness.

3.3. *Evidence from measurements under a bias electric field*

The dielectric spectrum evolves in a very characteristic way when a bias electric field is applied. From figure 5, it can be seen how the absorption peaks P_L and P_H first sharpen (without appreciable change in position) and then are more or less quenched out at sufficiently high field. In fact, the high frequency absorption vanishes completely at about 19 volts applied across the 2 μm cell (cf. figure 6 (*a*) and (*b*)), in good agreement with the value given by Chisso for the field-induced transition to the ferroelectric state. Hence, the P_H peak is related to the antiferroelectric order. The dielectric strength of the P_L peak is affected in a similar way, indicating a similarity in the aspect of molecular motion, but persists, with a lower value both in $\Delta\varepsilon_L$ and f_L, beyond the critical field for the antiferroelectric–ferroelectric transition. This means that P_L is related to a similar molecular reorientation, which is independent, except for the absolute value of $\Delta\varepsilon_L$ and f_L, on whether the molecules rotate as anti-tilt pairs or as single molecules in unison. The fact that the data in figures 5 and 6 have been taken at 30°C, i.e. 50 degrees below the transition to the C^*_α and A* phases, excludes that any of the peaks P_L and P_H may have anything to do with a soft mode, i.e. with fluctuations in θ. As $\Delta\varepsilon_H$ furthermore vanishes at the threshold field, the high frequency mode, in particular, cannot be a soft mode. Finally, the bias field would rapidly decrease the dielectric strength of a soft mode and not increase it, as is the case for both peaks.

3.4. *Our interpretation of the molecular aspect of the fluctuation processes*

As for the low frequency branch, we have been able to conclude that it can neither be attributed to any molecular reorientation around the short axis, nor to the soft mode, which is the corresponding collective motion. From the pronounced decrease in viscosity when the tilt angle θ gets very small see (figures 4 (*d*)), we may infer that this mode is a phase fluctuation around the cone, cf. figure 7. In the antiferroelectric state this motion may take place having

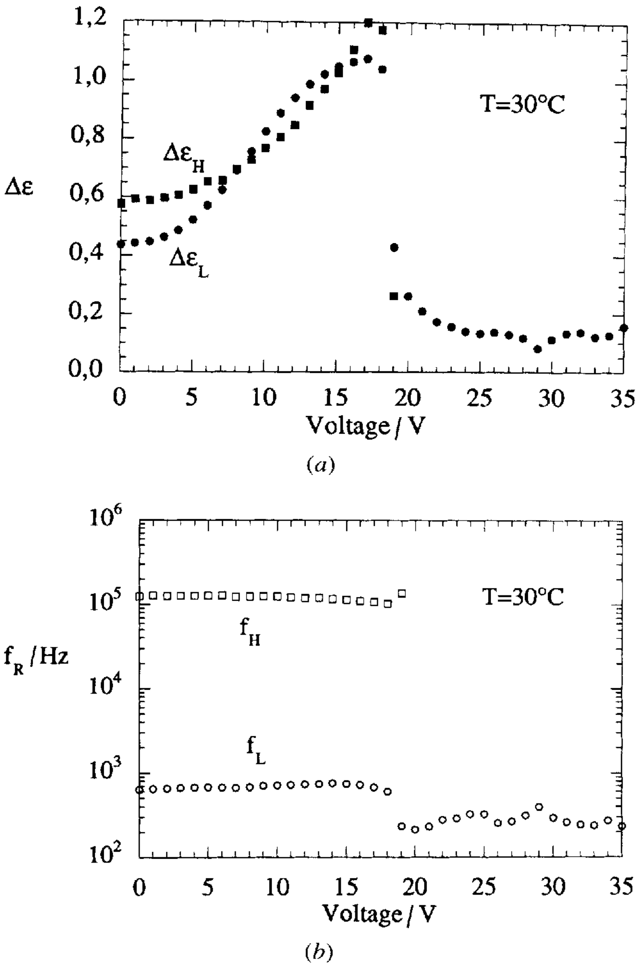

(*a*)

(*b*)

Figure 6. (*a*) Bias field dependence of the dielectric strength in the C^*_A phase. Note that the cell thickness is 2 μm. The threshold field for the antiferro- to ferro-electric transition is therefore around 9 V μm^{-1}. (*b*) Bias field dependence of the relaxation frequency in the C^*_A phase.

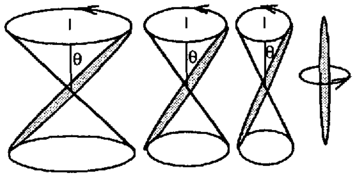

Figure 7. Phase fluctuations in the C^*_A phase. The viscosity for the cone motion varies as $\gamma_\varphi = \gamma_0 \sin^2\theta$ and thus can take on very small values as the tilt angle θ becomes small.

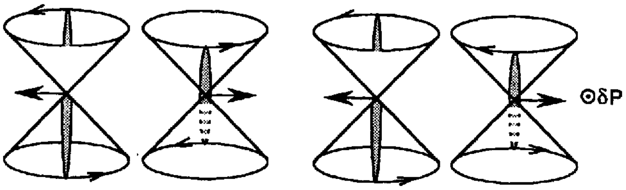

Figure 8. (*a*) In-phase motion of anti-tilt pairs. This kind of fluctuation does not let local polarization appear and cannot be seen dielectrically in this pure mode unless deformed by a helical superstructure. (*b*) Anti-phase fluctuation leading to the creation of a local polarization density $\delta\mathbf{P}$ in the direction illustrated.

the anti-tilt pairs moving *in phase* around the tilt cones, i.e. with the phase variable φ changing in the same sense, cf. figure 8 (*a*). Such as motion does not couple to an electric field and cannot be seen dielectrically. However, we know that a helicoidal superstructure exists in the C_A^* phase, with the anti-tilt pairs spiralling in a certain direction. The period of the helicoidal twist is very short, of the order of a fraction of a μm. Moreover, the φ difference of a pair is not quite 180°, so that there is a slight imbalance in the local polarization. Therefore a small residual polarization is spiralling along the superstructure. We believe that the low frequency mode is a phason fluctuation in this superstructure, i.e. a collective phase fluctuation where the molecules are moving essentially in phase. The bias field deforms and partially unwinds the helical superstructure. After the field-induced transition to the ferroelectric state the same motion now takes place with the molecules essentially parallel. The drop in frequency is natural because the anti-tilt motion in pairs corresponds to a higher value of elastic constant. The induced ferroelectric state may still possess the helical structure, perhaps strongly deformed, but not completely unwound.

The high frequency absorption, as concluded above, related to the antiferroelectric order and only exists as long as this order persists. In this case the molecules move against each other in their anti-tilt position, in anti-phase, i.e. with φ changing in opposite sense around the cones, cf. figure 8 (*b*). These fluctuations receive, in addition to the elastic torque, a restoring torque originating from the electric field energy when the dipoles do not any longer compensate each other locally, which explains the much higher frequency for the anti-phase fluctuations than for the in-phase fluctuations.

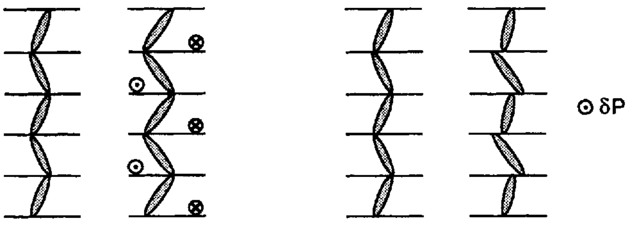

(*a*) (*b*)

Figure 9. (*a*) Tilt (soft mode) fluctuations which preserve local electrical neutrality, (*b*) tilt (soft mode) fluctuation leading to the appearance of a net polarization $\delta\mathbf{P}$ in the direction indicated. All molecules have been turned in a counter clock-wise sense and the anti-parallel polarization vectors in alternating layers do not any longer cancel.

As for the antiferroelectric soft mode, we may distinguish two modes, shown in figure 9. The figure 9 (*a*) shows fluctuations where the tilt increases or decreases by the same amount in alternating layers, such that no net polarization appears. Hence it does not couple to an electric field and cannot be seen dielectrically. In principle, there also exists an antiferroelectric soft mode which we have illustrated in figure 9 (*b*). This mode is connected to the appearance of an unbalanced polarization of a direction indicated in the figure. Consequently, the same distortion, which macroscopically means a deviation in the optic axis, should be excited by a electric field applied in the same direction. We would at least have detected this mode after quenching out the phason (or Goldstone-like) modes, whose amplitudes anyway are much smaller than in the ferroelectric case, as described above by the bias field. However, we did not, and hence conclude that it does not exist, i.e. its excitation amplitude can be neglected. Evidently, the anti-phase mode takes up the corresponding response to an external field, equivalent to a field-induced deviation in the optic axis.

We are grateful to Chisso Corporation, Japan, for providing a sample of the antiferroelectric material. This work was supported by the Swedish Natural Science Foundation, and the Swedish National Board for Technical Development.

References

[1] Ostrovski, B. I., Rabinovich, A. Z., Sonin, A. S., Strukov, B. A., and Taraskin, S. A., 1978, *Ferroelectrics*, **20**, 189.

[2] Hoffmann, J., Kuczynski, W., and Malecki, J., 1978, *Molec. Crystals liq. Crystals*, **44**, 287.

[3] Benguigui, L., 1982, *J. Physique*, **43**, 915.

[4] Glogarova, M., Fousek, J., Lejcek, L., and Pave, J., 1984, *Ferroelectrics*, **58**, 161.

[5] Blinc, R., and Zeks, B., 1978, *Phys. Rev. A*, **18**, 740.

[6] Martinot-Lagard, Ph., and Durand, G., 1981, *J. Physique*, **42**, 269.

[7] Bahr, Ch., Heppke, G., and Sharma, N. K., 1987, *Ferroelectrics*, **76**, 151.

[8] Filipic, C., Carlsson, T., Levstik, A., Zeks, B., Blinc, R., Gouda, F., Lagerwall, S. T., and Skarp, K., 1988, *Phys. Rev. A*, **38**, 5833.

[9] Birdar, A. M., Wrobel, S., and Haase, W., 1989, *Phys. Rev. A*, **39**, 2693.

[10] Kremer, F., Schönfeld, A., Hofman, A., Zentel, R., and Poths, H., 1992, *Polym. Adv. Techn.*, **3**, 249.

[11] Hiraoka, K., Taguchi, A., Ouchi, Y., Takezoe, H., and Fukuda, A., 1990, *Japan J. appl. Phys.*, **29,** L103.

[12] Isozaki, T., Suzuki, Y., Kawamura, I., Mori, K., Yamada, N., Orihara, H., and Ishibashi, Y., 1991, *Japan J. appl. Phys.*, **30,** L1573.

[13] Okabe, N., Suzuki, Y., Kawamura, I., Isozaki, T., Takezoe, H., and Fukuda, A., 1992, *Japan J. appl. Phys.*, **31,** L793.

[14] Glogarova, M., Sverenyak, H., Nguyen, H. T., and Destrade, Ch., 1993, *Ferroelectrics*, **147,** 43.

[15] Gisse, P., Pavel, J., Nguyen, H. T., and Lorman, V. L., 1993, *Ferroelectrics*, **147,** 27.

[16] Moritake, H., Uchiyama, Y., Myojin, K., Ozaki, M., and Yoshino, K., 1993, *Ferroelectrics*, **147,** 53.

[17] Hiraoka, K., Takezoe, H., and Fukada, A., 1993, *Ferroelectrics*, **147,** 13.

[18] Cepic, M., Heppke, G., Hollidt, J.-M., Lötzsch, D., and Zeks, B., 1993, *Ferroelectrics*, **147,** 159.

[19] Lorman, V. L., Bulbitch, A. A., and Toledano, P., 1994, *Phys. Rev. E*, **49,** 1367.

[20] Gouda, F., Skarp, K., and Lagerwall, S. T., 1991, *Ferroelectrics*, **113,** 165.

[21] Kilian, D., Hiller, S., Goodby, J. W., Nishiyama, I., Pikin, S. A., and Hasse, W., 1994, *15th International Liquid Crystal Conference* (Poster J-Sbp4), Budapest 1994.